JCTC Journal of Chemical Theory and Computation

Article

pubs.acs.org/JCTC

# Sidekick for Membrane Simulations: Automated Ensemble Molecular Dynamics Simulations of Transmembrane Helices

Benjamin A. Hall,† Khairul Bariyyah Abd Halim, Amanda Buyan, Beatrice Emmanouil, and Mark S. P. Sansom*

Department of Biochemistry, University of Oxford, South Parks Road, Oxford OX1 3QU, United Kingdom

Supporting Information

**ABSTRACT:** The interactions of transmembrane (TM) $\alpha$-helices with the phospholipid membrane and with one another are central to understanding the structure and stability of integral membrane proteins. These interactions may be analyzed via coarse grained molecular dynamics (CGMD) simulations. To obtain statistically meaningful analysis of TM helix interactions, large (N ca. 100) ensembles of CGMD simulations are needed. To facilitate the running and analysis of such ensembles of simulations, we have developed Sidekick, an automated pipeline software for performing high throughput CGMD simulations of $\alpha$-helical peptides in lipid bilayer membranes. Through an end-to-end approach, which takes as input a helix sequence and outputs analytical metrics derived from CGMD simulations, we are able to predict the orientation and likelihood of insertion into a lipid bilayer of a given helix of a family of helix sequences. We illustrate this software via analyses of insertion into a membrane of short hydrophobic TM helices containing a single cationic arginine residue positioned at different positions along the length of the helix. From analyses of these ensembles of simulations, we estimate apparent energy barriers to insertion which are comparable to experimentally determined values. In a second application, we use CGMD simulations to examine the self-assembly of dimers of TM helices from the ErbB1 receptor tyrosine kinase and analyze the numbers of simulation repeats necessary to obtain convergence of simple descriptors of the mode of packing of the two helices within a dimer. Our approach offers a proof-of-principle platform for the further employment of automation in large ensemble CGMD simulations of membrane proteins.

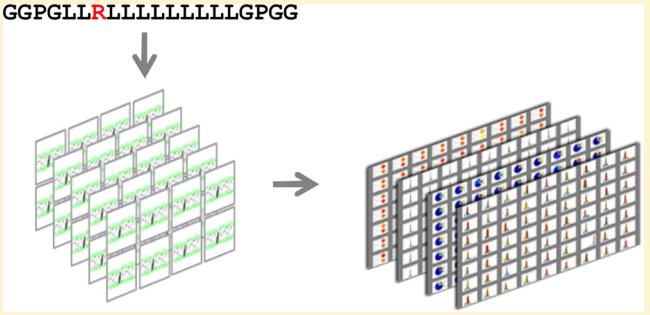


## INTRODUCTION

Molecular dynamics (MD) has been used extensively to understand the structure and dynamics of a wide range of different systems, providing dynamic structural insights into behavior on experimentally inaccessible time- and length scales.[1−5] With increasing computing power and sophistication, the complexity of systems studied has increased, leading to the application of semiautomated workflows[6] and of high throughput (HT) approaches for performing large comparative analyses of multiple systems.[7,8] HT workflows have been applied widely to docking problems[9−11] and are increasingly being applied to MD simulations.[12] However, such workflows typically have several manual steps (see the workflow in Figure 1), which are both laborious and can potentially introduce variation in the simulation protocol. Alongside this growth in HT approaches, the ongoing successes of MD approaches and related techniques to modeling biomolecular systems has led to the development of multiple different approaches to automating specific workflows through user-friendly interfaces for performing simulations.[13] This in turn has driven the development of Web interfaces allowing outside users to access and use data from the simulations in an accessible form for both specialists and nonspecialists.[7,14,15]

High throughput approaches also pose novel issues for data management and analysis. When comparisons between multiple systems are considered (alongside simulation repeats for statistical confidence), these can create problems in terms of simulation and data management from the sheer size and number of individual systems, further slowing the analysis. The MD simulations themselves are computationally intensive, frequently requiring supercomputer time to generate useful data for large systems. Simulation software (such as GROMACS,[16] NAMD,[17] Charmm,[18] GROMOS[19] and AMBER[20]) typically manage scaling over large numbers of processers, and while this is becoming increasingly optimized, scaling can break down for small systems and extremely large numbers of processors.[16] Coarse grained (CG) simulations increase simulation speed and improve scaling through the use of a simplified description of the system, at the cost of some loss of detail,[21−23] but still suffer from many of the other disadvantages in terms of setup and analysis.

Here, we present the Sidekick software, a grid application that addresses the challenges posed by manual setup,

Received: January 3, 2014
Published: April 7, 2014





dx.doi.org/10.1021/ct500003g | J. Chem. Theory Comput. 2014, 10, 2165−2175

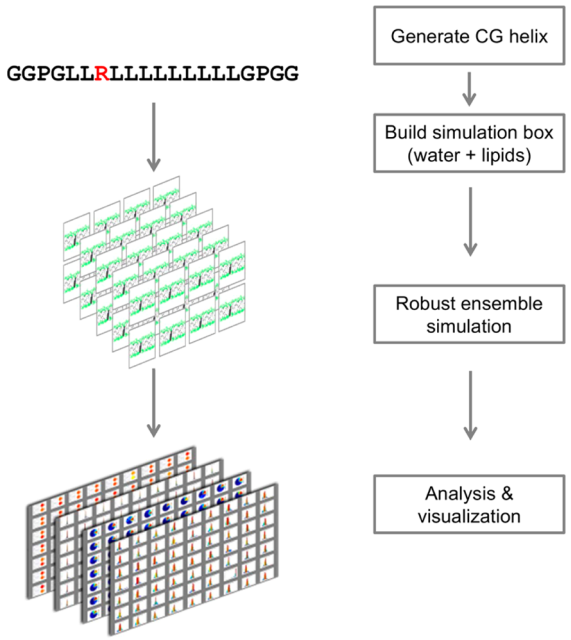


**Figure 1.** Schematic of a Sidekick pipeline. A single script runs an ensemble of simulations from a handful of input values, including the amino acid sequence of a helix, the force field, and a random seed. From this, a CG model of an $\alpha$-helix is built, it is placed in a box with randomly placed water, lipids, and counterions, and an ensemble of molecular dynamics simulation is performed. The resulting trajectories are visualized and analyzed in terms of, e.g., the helix depth in the membrane, helix tilt angle, and helix screw rotation angle.

simulation, and data management, and scaling for CGMD simulations of helices in a bilayer through deep automation. From an input sequence or set of sequences, entered through a command line interface or Web page, simulation systems are built, simulations run, and analysis performed on the resulting trajectories before being stored in an ordered file structure on a central server. Simulations are performed in replicate (typically >100 times each) on single processors, giving excellent sampling and creating an "embarrassingly parallelizable" problem which scales perfectly across the computing resource. Sidekick itself is a collection of python scripts and modules, which either individually perform distinct steps in the pipeline or execute external applications (e.g., GROMACS commands). Ensembles of pipelines are performed over a mixed grid/cluster setup, consisting of a mixture of machines, including a dedicated cluster as well as underused workstations (totaling in excess of 300 processors). Job management is performed using Xgrid software, and data are shared using NFS (both available as part of the operating system). Raw data is available for detailed analysis across the ensemble of simulations that are generated, alongside Web interfaces, describing peptide properties based on key metrics (described below). The application of grid based technologies here follows a different approach from that taken in a wide range of disciplines, including the Seti@home,[24] folding@home,[25] "screensaver lifesaver"[10] (each dedicated to a specific research focus), the UK National Grid Service, and OpenMacGrid (general use grids). Our approach is necessarily different from these, due to the computational time required to perform the simulations, and the storage and transport requirements created by large, continuous MD trajectories. In contrast to high throughput approaches driven by specific tasks such as calculating the PMF of drug binding[26] or the calculation of whole protein dynamics (e.g., Copernicus[27]), Sidekick is focused on calculating and presenting a heavily sampled description of the behavior of transmembrane (TM) helices at equilibrium.

To date, we have used this software to aid our understanding of NMR data on model peptides,[28,29] of high throughput experimental assays,[30] of bacterial signaling systems,[31] and of fusion peptides.[32,33] Over four years, the application of this approach by ~10 users in our group has generated over 5 TB of data and used ~1,000,000 CPU hours, and the size of the grid/cluster has been upgraded several times to take this into account. The highly modular approach taken in writing the code has allowed for new features to be added rapidly (including changing starting configurations, adding umbrella potentials, and inline force field modification). This increases the potential for development of the code in future for novel purposes, and as such, we regard Sidekick as both a tool in itself and also as a framework for future tool development.

Here, we validate the software by calculating the likelihood of arginine residue "guests" in "host" hydrophobic helices to insert into a phospholipid bilayer. We take 2 related helix systems, which have been explored experimentally: poly leucine helices of lengths 11 and 12 (here referred to as pL11 and pL12). The energy of insertion is found to be ~1 kCal/mol, consistent with energies measured experimentally in the refolding and insertion of OmpLA[34] and insertion of helices by the translocon apparatus,[35] and compatible with equilibrium calculations of peptide insertion in all atom simulations.[36] We further use the pipeline technology to explore the association of ErbB1 TM helix dimers in a DPPC membrane. We analyze convergence of the helix packing modes and show that the major packing mode predicted is in agreement with a recent NMR structure[37] of the ErbB1 TM helix dimer.

## METHODS

**Core Software.** Individual Sidekick pipelines are based on GROMACS (www.gromacs.org), python, and numpy. Optionally, matplotlib can be used to generate plots for each individual run. The management of simulations across the cluster is controlled through Xgrid in our implementation, though other grid managers (such as SGE) have been used successfully. Data (in terms of software and outputs) is stored on a file server and in our implementation shared using NFS, though this is performed at the level of the operating system and must be set up manually for each "agent" running the pipelines. Analysis is performed using custom analysis code written in python and numpy. To ensure faithful reproduction of different coarse grained force fields, the unmodified relevant scripts are run within the pipeline. Specifically, GROMACS tools editconf/trjconv are used for structure/trajectory manipulation, grompp/mdrun for simulation (and preprocessing), genbox for solvation, and genion for the addition of ions. Sidekick is available from http://sbcb.bioch.ox.ac.uk/Sidekick/.

**Single Helix Simulation Pipelines.** Individual simulations are performed within independent automated pipelines, wherefrom the input sequence and options are used to generate a CG $\alpha$-helix, a water/lipid system (with counterions), and perform the simulation (Figure 1). An individual pipeline is started using the script CG_Helix.py and can be run outside of the ensemble for testing purposes. The individual pipelines allow for a selection of a wide variety of different aspects of the simulation (see Table 1 for all options). Key parameters for all simulations include the choice between different force fields

**Table 1. Options for Running an Individual Simulation Pipeline**

| option | default | effect |
|---|---|---|
| -t, --type | MARTINI | specifies which forcefield or version of the forcefield to use |
| -j, --job_name | | specifies the location of the results |
| -b, --batch-mode | false | instructs the pipeline to store the resulting files on the file server |
| -s, --sequence | | sequence used to build the helix |
| -l, --length | 100 ns | simulation length |
| -u, --unbias | false | use a cubic box with lipids distributed evenly across the box; simulations to be run with anisotropic pressure coupling |
| -r, --random-seed | 5 | seed used to generate initial velocities |
| --randomize_lipids | false | use the seed to generate different lipid configurations across the ensemble |
| -a, --angle | 0 | initial angle of the peptide relative to the $z$ axis |
| --change_temperature | 323 | temperature for the simulation |
| -p, --position | 0 | initial z position of the peptide in the box, relative to the center of the box |
| --system_size | "XS" | preselected box system sizes and numbers of lipids; "XS" contains 128 lipids, "S" 256 lipids |
| --preformed_bilayer | false | use a preformed bilayer rather than self-assembly |
| --special | | additional options to pass to the CG scripts |
| --lipid_headgroup_mix | DPPC | mixture of lipids to be used in the simulation; type and ratio are specified |
| --wallclock | 48 | maximum length MD simulations should run |

(either the "Bond"[21] or MARTINI[23] CG force fields) and different available versions of force fields, system size (selected from predefined system sizes), and initial lipid configurations. The default behavior is to build a system consisting of a DPPC/water/counterion system around the peptide, with a cuboid box $7 \times 7 \times 15$ nm$^3$ where lipids are located in a narrow section in the center of the box, and to use semi-isotropic pressure coupling when performing the simulation (coupling XY and Z separately). This helps ensure that the bilayer is formed in the XY plane and within the first 10−20 ns. Alternatively, a preformed bilayer can be used (with semi-isotropic pressure coupling) or the system can be built as a $9 \times 9 \times 9$ nm$^3$ cube with lipids evenly distributed throughout the box, and the pressure coupled anisotropically (i.e., coupling X, Y, and Z separately), when the "--unbias" option is enabled. The three system configurations alter the behaviour and reliability of the simulations to give stable bilayers in any plane; 100 % of preformed bilayers remain stable, ∼95 % of "biased" bilayers form stably in the XY plane, and ∼75% of unbiased self-assembly protocols form bilayers in the XY, YZ, or XZ planes.

Simulation run files are generated based on the input options and a set of standard template run files, which are used to generate the desired system configurations for each simulation. Independence of each run is achieved by altering the starting seed for the generation of velocities in each simulation. However, if the user wishes, it is further possible to vary the systems, either by altering the position and angle of the peptide (which by default is located in the center of the box and aligned to the Z axis) and by using the seed for each run to seed the positioning of lipids performed by genbox. Alteration of the peptide position and orientation are of particular value when using preformed bilayers. Temperature and pressure are coupled at 323 K and 1 bar using the Berendsen[38] weak coupling algorithm ($\tau_T$ = 1 ps and $\tau_P$ = 10 ps). The compressibility is set at $3 \times 10^5$ (1/bar).

Individual pipelines are designed to be robust through the use of (a) wall clocks and (b) automatic restarts with a shorter time step (Figure 2). The purpose of these is to mimic the typical CGMD workflow while ensuring that simulations stuck in unproductive states are cleared from the cluster to allow new simulations to run. The wall clock ensures that jobs that stop generating data but remain running indefinitely do not block compute resources, which can lead to a net reduction in grid performance over time. The reduction of the time step reflects the lack of knowledge *a priori* regarding the selection of an appropriate time step in coarse grain simulations (for extensive discussion, see refs 39 and 40). On completion of mdrun, we tested output trajectories and logs for successful termination. If this has not occurred, the time step is reduced (from 20 to 10 fs), and the simulation is restarted from the last frame for which position and velocity have been collected. The resulting trajectories are concatenated at the end of the pipeline prior to analysis. Such crashes are relatively rare and at least partially system dependent.

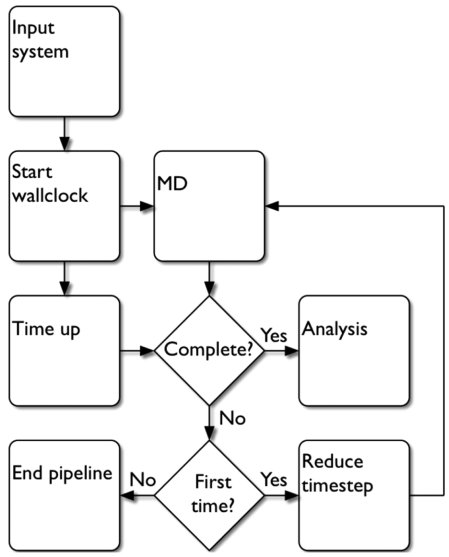


**Figure 2.** "Robust" simulation flowchart. Initially, a wall clock is started to ensure that individual pipelines do not become halted where calculations become trapped in an unproductive infinite loop. Subsequently, CG simulations are started with a time step of 20 fs. Once the simulation finishes (either due to correct completion or crash), or the wall clock runs out, the resulting files are tested for simulation completion. If no crashes have occurred, the resulting trajectories are analyzed. If the simulation has crashed, and if this is the first crash, the time step is reduced to 10 fs, and the simulation is restarted from the last stored frame with positions and velocities. If the simulation has crashed once before, the pipeline ends.

**Multiple Helix Pipelines.** Simulation pipelines also exist to predict the behavior of systems with multiple helices.[41] These are always performed using a preformed bilayer, in order to specify helix orientation, and the user is currently limited to using DPPC, DPPE, and DPPG lipid mixes. Simulations are performed as described for single helices, and individual helices in the simulations are analyzed using the same metrics (position, tilt, and rotation) in addition to new metrics specific to pairwise helix interactions. These new metrics include

relative positions of helices, helix contact analyses, and termini-to-termini distance (useful when considering helices which are normally connected by a flexible linker region).

The extension of the approach to multihelix systems is supported by the extensive use of object oriented programming and specifically the reuse of large sections of the code by inheritance, allowing common functions to be shared between the different use cases. Furthermore, the code is designed to be highly modular, with discrete functions in the code (e.g., system generation, MD simulation, etc.) designed to be easily reused in a new code.

**Grid Architecture and Sidekick Ensembles.** Simulations are performed across a hybrid grid/cluster architecture (see Supporting Information, Figure S1). Individual pipelines run independently and on single cores and as such do not require fast networking, and by default, single helix simulations write data locally, only transferring output data to the central file server at the finish of the pipeline. A mixture of dedicated cluster nodes and idle workstations are used to perform calculations connected to the controller and central file server by wired or wireless networking. However, access to the core software and the centralized data store is achieved through NFS, reflecting the practical issues with sharing software and output data across a typical grid setup. As such, we refer to our architecture as hybrid grid/cluster as it has features of both HPC paradigms.

Machines can be classed as agents, headnodes, and clients depending on their specific functionality. Agents perform simulations as instructed by the grid manager. Headnode tasks (serving files, managing the cluster, and presenting a Web server interface to the data) can be centralized on a single machine or split between multiple machines; the cluster manager and file server need direct access to the agents, and the Web server needs direct access to the file server and cluster manager for submitting and retrieving job information. Finally, client machines submit jobs and retrieve data, either through a command line interface or through the Web site (complete data retrieval is only possible from the command line). Agents can write output data locally and either copy to the file server on completion or write directly to the file server. When data are written locally by the agents, network speeds do not pose a bottleneck for the pipelines, allowing agents to perform simulations over slower networks (e.g., wireless). The concurrent transfer of data from multiple agents, however, can lead to network congestion, causing problems relating to Xgrid communication. To prevent this, we can switch the pipeline to writing centrally. While this presents the possibility of reduced performance, no notable slow-downs were found when using gigabit ethernet.

In our implementation, an Xgrid controller initially accepts a batch file (in XML) describing all individual pipelines to be run (Figure 3). This is generated programmatically, but for SGE, job array scripts can be written by hand to generate the ensemble. In principle, this approach could be applied to cloud resources where a MapReduce model[42] could be employed to perform and aggregate the pipeline and outputs. The controller instructs agents (slave nodes in SGE) to perform individual pipelined simulations, which read software from the centralized file server and at the end of a pipeline copy data to the central datastore. Finally, users can view graphics rendered in javascript/HTML5 through the Web server describing the metrics of individual sequences over their ensemble, or the complete output can be accessed through the command line.

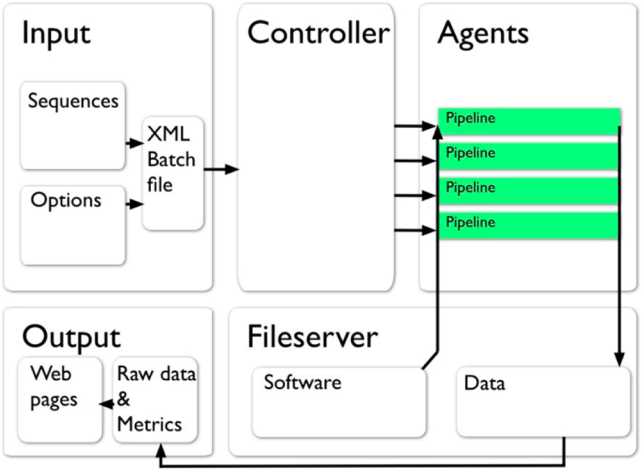


**Figure 3.** Schematic of the ensemble simulation workflow (arrows represent the flow and transformation of information at distinct stages of the ensemble). To generate an ensemble of Sidekick jobs, a collection of helix amino acid sequences and simulation options (e.g., number of jobs, choice of force field, etc.) is used to generate an XML input file for submission to the controller, a machine which coordinates jobs across the grid. From this file, the controller starts jobs on all available "agents", which run individual pipelines, reading required software from a centralized file server and depositing output files onto the same file server. Files may be written locally during the simulation and copied at the end of the job or written as the job is running. Individual simulations are analyzed within each pipeline to generate metrics to describe the orientation of the helix over the course of the simulation. Both raw data (trajectories and other outputs) and descriptive metrics (e.g., the position and orientation of the helix in the membrane) can be accessed on the file server or presented through a Web interface.

The ensemble size is limited by available resources (storage and compute). Ensembles up to ∼12,000 simulations have been performed.

**Simulations Presented Here.** CGMD simulations of the helices in ∼128 lipid DPPC bilayer were performed using a membrane self-assembly protocol successfully employed in the past for single TM helices[30]and for more complex membrane proteins.[21] Sequences of each peptide used here are given in Table 2. Simulations are performed using Gromacs v3.[43] The unbiased simulation protocol was followed (where the box is cubic, and the pressure is coupled anisotropically), and the temperature was coupled at 323 K. About 400 simulations were performed for each helix sequence.

In single helix simulations presented here, we have used a local modification of the MARTINI force field[23,44] (the "Bond" force field), following the protocol used previously for predicting translocon mediated insertion.[30] The MARTINI approach reduces system size from ∼4 non-hydrogen atoms to a single coarse grained particle. Lennard-Jones interactions between particles are calculated based on 5 interaction levels between 4 classes of particle. These classes reflect polar, charged, mixed polar/apolar and apolar characters, where mixed and charged particle types are further divided into 5 and 4 subclasses, respectively, to reflect hydrogen bonding capabilities. Lennard-Jones interactions were shifted to zero between 0.9 and 1.2 nm. Electrostatic interactions are treated Coloumbically and were shifted to zero between 0 and 1.2 nm. The peptide backbone in the helix is originally generated from an ideal all atom $\alpha$-helix and converted to its coarse

Table 2. Model Hydrophobic Helix Sequences[a]

| L11 Series |
|---|
| GGPGLLLLLLLLLLGPGG |
| GGPGLLLLLLLLLLRGPGG |
| GGPGLLLLLLLLLRLGPGG |
| GGPGLLLLLLLLRLLGPGG |
| GGPGLLLLLLLRLLLGPGG |
| GGPGLLLLLLRLLLLGPGG |
| GGPGLLLLLRLLLLLGPGG |
| GGPGLLLLRLLLLLLGPGG |
| GGPGLLLRLLLLLLLGPGG |
| GGPGLLRLLLLLLLLGPGG |
| GGPGLRLLLLLLLLLGPGG |
| GGPGRLLLLLLLLLLGPGG |
| **L12 Series** |
| GGPGLLLLLLLLLLLLGPGG |
| GGPGLLLLLLLLLLLRGPGG |
| GGPGLLLLLLLLLLRLLGPGG |
| GGPGLLLLLLLLRLLLLGPGG |
| GGPGLLLLLLLRLLLLLGPGG |
| GGPGLLLLLLRLLLLLLGPGG |
| GGPGLLLLLRLLLLLLLGPGG |
| GGPGLLLLRLLLLLLLLGPGG |
| GGPGLLRLLLLLLLLLLGPGG |
| GGPGRLLLLLLLLLLLLGPGG |

[a]For each series, the "parent" hydrophobic sequence is shown followed by a set of sequences in which the arginine residues are progressively moved along the hydrophobic core sequence.

grained representation. Helicity is maintained in the peptide backbone through harmonic restraints between hydrogen bonded particles.

For simulations of ErbB1 TM helix dimerization, we use the same force field and simulation parameters as for single helix simulations. Two parallel helices are inserted into a preformed DPPC membrane, separated from one another by ∼5 nm. 50 × 500 ns simulations were performed of helix pairs in total.

**Analysis of Helix Dimer Packing Interactions.** TM helix dimers were characterized in terms of their helix crossing angles. The Cα coordinates of each helix and their respective centroids were calculated in each frame of a given trajectory. If the distance between helix centroids exceeded 1 nm, the frame was skipped as the helices were considered not to be packed against one another. Otherwise, the first eigenvector of each helix was calculated, and the magnitude of the crossing angle was determined using the cross-product of the helices' eigenvectors. To determine its handedness using the standard conventions,[45] the helices were rotated so the first helix was aligned to the +$x$-axis. New eigenvectors were calculated, and their cross-product was determined and aligned with the +$x$-axis. The orientation of the eigenvector through the first helix along the $z$-axis and the $x$-component of its centroid determined the handedness of the angle.

An iterative jackknife approach[46,47] was used for assessing the convergence of the crossing angle distributions and of the helix contact residues. This technique allowed the sampling of the whole range of possible subset sizes. It has also been demonstrated that randomly choosing a small number (e.g., 1000) of the total possible combinations is sufficient for sampling purposes.[46] This is necessary because as the number of simulations increases, the number of possible combinations per subset sizes increases such that it becomes unachievable to sample all possible combinations.

To assess the convergence of the list of interhelix contact residues, for each chosen subset, all distance matrices from all of the frames of the simulations were averaged together to give an overall distance matrix. Then, for each of the chosen subsets, the six residues which have the lowest Cα distances are tallied and put together into an overall matrix. This overall matrix holds the frequency of the closest contacts that appear in the subsets of the simulations, generating an overall heat map for contacting residues. This is done for each subset size.

## RESULTS AND DISCUSSION

**Performance of the Pipeline.** We have evaluated the Sidekick approach via two examples of TM systems which benefit from automated running and analysis of ensembles of simulations: (i) insertion of single TM helices into a bilayer, running and analyzing ca. 8000 simulations with a total CG simulation time of ca. 0.8 ms; and (ii) dimerization of TM helices in a preformed lipid bilayer, analyzing the convergence of the predicted helix packing as a function of ensemble size.

**Single TM Helix Insertion.** One major use of Sidekick is to investigate the probabilities of insertion of TM helices into a lipid bilayer. This is of interest in contributing to an understanding of the factors which influence the stability and structure of membrane proteins.[48,49] There have been a number of biochemical[35,50] and biophysical[51,52] studies of this problem, and it has also been the subject of a number of computational studies, including both CG[30,53] and atomistic[36,54] MD simulations. Of particular interest is the thermodynamics of insertion of otherwise hydrophobic TM helices containing a cationic arginine side chain.[55−58] It has been shown that although complete burial of a cationic side chain within the hydrophobic core of a bilayer is unfavorable, local distortion of the bilayer and "snorkeling" of the arginine side chain may occur so the cationic moiety of the side chain is able to form favorable electrostatic interactions with anionic phosphates of the lipid headgroups. We have previously shown that the insertion energies of peptides into the membrane may be accurately estimated using ∼400 simulations.[30]

To evaluate the positional dependence of the insertion of Arg-containing TM helices in a bilayer, there have been experimental studies whereby the length of a model hydrophobic TM helix is "scanned" with a single Arg residue and the effect of the cationic side chain on the insertion propensity of the TM helix evaluated.[49] We have therefore used Sidekick to generate a large (ca. 8000) ensemble of simulations, scanning an Arg along two hydrophobic helices of differing length, and performing TM helix/lipid bilayer self-assembly simulations to evaluate profiles for the insertion thermodynamics of the helices.

Simulations of Arg "guest" residues at different positions along two leucine-containing "host" helices were performed. The two systems containing either 11 or 12 leucines form the hydrophobic cores of 19- or 20-mer helices (Table 2). The two "host" helices were selected based on their relative insertion energies into a DPPC bilayer such that the L11 helix marginally favors an interfacial orientation, while the L12 helix favors a transmembrane orientation. As such, these two families of helices may be expected to be sensitive to the introduction of a single arginine.

For each ensemble of simulations, an individual simulation was run from an initially random arrangement of lipids in a box also containing the helix and waters. The lipids self-assemble to form a bilayer, with the helix adopting a TM and/or a surface orientation (Figure 4; also see Supporting Information, Movie 1). For each helix sequence, an ensemble of ca. 400 simulations each of duration 100 ns was performed.

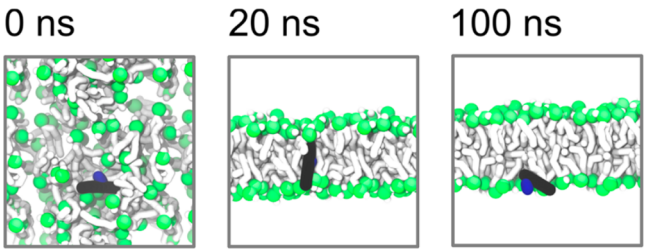


**Figure 4.** Dynamics of a single helix insertion simulation illustrated for an L11 helix (see main text and Table 1). Snapshots are shown from a single simulation pipeline at 0, 20, and 100 ns. Lipids are rendered as gray tubes with green spheres for phosphate particles. The helix backbone is rendered as a black tube and the arginine side chain rendered in blue. At 20 ns, a bilayer has formed, with the peptide in a transmembrane orientation, but between 20 and 100 ns, the helix exits the bilayer and remains interfacial for the remainder of the simulation. The entire trajectory is shown in Supporting Information, Movie 1.

Sidekick was used to analyze the position and orientation of the helix relative to the bilayer over the length of the trajectory. Thus, each output trajectory of an ensemble of runs was analyzed in terms of helix position relative to the center of the membrane, helix tilt angle in the membrane, and the azimuthal rotation of the helix in the membrane (that is, the rotation angle around the helix axis, also referred to as the direction of tilt) (Figure 5A). The percentage of helix insertion in the bilayer is quantified based on helix tilt and the depth of the helix in the bilayer. Finally, the end state of the bilayer is assessed to determine its location and whether the bilayer has formed a continuous sheet. In addition to writing the specific metric values over time to file, a summary file with information on the end state and percentage insertion is also generated to aid subsequent filtering of data and ensembles.

For each time point in the simulation, a helix is defined as transmembrane or not transmembrane based on the tilt angle and depth of the helix in the membrane (Figure 5B). Specifically, if the center of mass of the helix backbone is within 1 nm of the center of mass of the bilayer core (along the axis of the bilayer normal) and the helix tilt angle is less than 65° relative to the bilayer normal, the helix is considered to be inserted in the membrane. The (apparent) free energy of insertion of a helix across the ensemble is calculated based on the percentages of time in inserted and noninserted states. The free energy of insertion is defined as

$$\Delta G_{\mathrm{APP}} = -RT \ln K$$

where

$$K = \%(\text{inserted})/\%(\text{not-inserted})$$

This is intended to match the definition used in experimental studies[50] where the % (inserted) and % (not-inserted) are calculated from the percentage of single glycosylation events relative to double glycosylation events following translocon-mediated insertion.

To calculate an energy profile for insertion of an arginine residue at different positions in the host hydrophobic helix, we place arginine residues at different positions in the sequence (Table 2) and compare the change in energy relative to the purely hydrophobic host helix (Figure 6). The resultant profiles are similar for both the L11 and L12 hosts with the important difference that the baseline profile is overall favorable for TM insertion for the L12 host. In each case, the peak in the profile is for an Arg residue in the center of the helix in which location it is unable to effectively snorkel to headgroup phosphates on either side of the bilayer in order to stabilize TM orientation of the helix.

This result is consistent with our previous results based on CFTR-derived helices, which predicted an energy barrier within an order of magnitude of the experimentally determined values from translocon-mediated helix insertion experiments[35,50] and with refolding experiments of the membrane protein OmpLA.[34] Furthermore, these values are consistent with results from all atom simulations at equilibrium.[36]

**ErbB1 TM Helix Dimerization.** As a second example of the use of Sidekick to enable the running and analysis of an ensemble of TM helix simulations, we have investigated the dimerization of a CG model of the TM helix domain from the ErbB1 receptor. ErbB1 belongs to the ErbB family of receptor tyrosine kinases, which is important in the regulation of cell growth, differentiation, and migration. Aberrant signaling by ErbB1 is associated with various cancers.[59,60] The TM region of ErbB1 contains two small-$x_3$-small motifs,[61] one toward its N-terminus and one toward its C-terminus. A recent study by Endres et al.[37] has shown the TM region of the ErbB1 is crucial for the activation of the receptor as the intracellular domain alone is monomeric and incapable of independent dimerization. Using an NMR based approach, they showed that the ErB1 TM-juxtamembrane (TM-JM) region formed a contact at the N-terminus with a crossing angle of $\sim -44°$, corresponding to a right-handed packing of the TM helices.[37] This packing is mediated via the N-terminal TGxxGA sequence motif and is required for the correct orientation of the JM region and thus the activation of the receptor. They further showed that mutation of the motif to poly isoleucine results in significant inhibition of the receptor. We therefore wished to explore the dimerization of the TM helices of ErbB1 in CG simulations, in

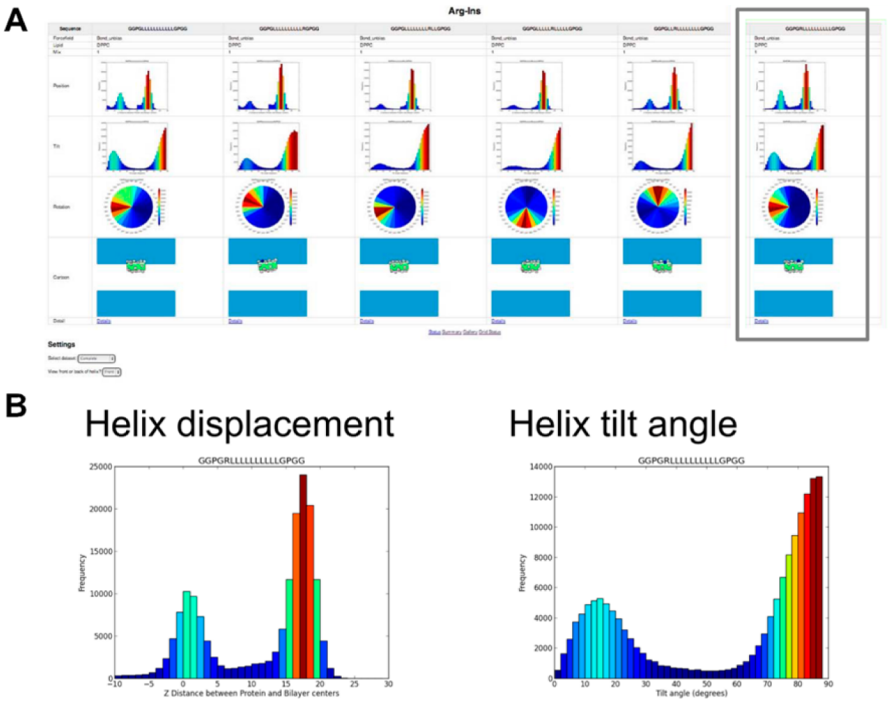


**Figure 5.** Analysis of a single helix insertion simulation ensemble. Panel A shows part of a screen snapshot from an analysis of an ensemble of single helix insertion simulations. Panel B shows the helix displacement and helix tilt angle distributions for a single sequence from that ensemble.

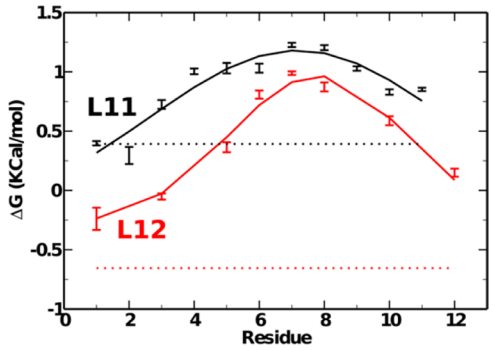


**Figure 6.** Insertion free energies of the model hydrophobic helices of the L11 and L12 series (see Table 1) with arginine at different positions along the peptide length (shown on the *x*-axis). The energies of the purely hydrophobic L11 and L12 "parent" sequences are plotted as broken horizontal black and red lines for comparison. Free energies of insertion were calculated as $\Delta G = -RT \ln K$ where K = % (inserted)/% (not-inserted). Ensembles of ca. 400 simulations were run for each sequence.

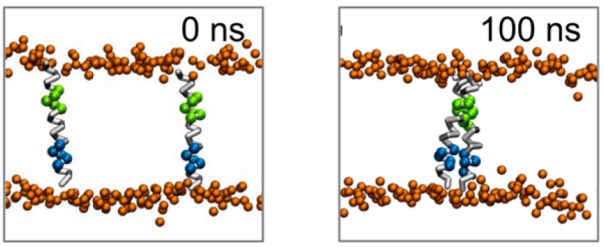


**Figure 7.** Simulations of ErbB1 TM helix dimerization. Snapshots of a single simulation at 0 and 500 ns showing the two helices inserted in a lipid bilayer. Phosphate groups of the phospholipids are shown as orange spheres, TM helix backbones as white chains, with the N- and C- terminal regions rendered in green and blue, respectively. The two helices associate spontaneously to form a specific interaction around the N-terminal motif.

particular to analyze the size of the simulation ensemble required for reasonable convergence to a structure compatible with the existing experimental[37,62] and computational (e.g., refs 63 and 64) data.

To this end, two ErbB1 TM helices were preinserted in a DPPC bilayer at an initial separation of ∼6 nm. This system was used to initiate an ensemble of 50 × 500 ns helix dimerization simulations performed using the Sidekick pipeline. In simulations, in each case the helices were observed to spontaneously associate during the simulations from their initial separated configuration (Figure 7).

The ensemble of 50 dimerization simulations was analyzed in terms of the helix crossing angle distributions as these allow for ready identification of the frequency of formation of right-handed (i.e., negative crossing angle) helix dimers. Right-handed packing of TM helices is characteristic of interactions via a small-$x_3$-small sequence motif,[61] as exemplified by glycophorin.[65] The full ensemble of 50 simulations showed a strong preference for right-handed packing of the ErbB1 TM helices, in agreement with NMR structures (Figure 8A). We therefore used this ensemble to explore convergence of the simulations to this characteristic structure. Our first pass at such analysis consisted of randomly selecting a single subset of 5, of 10, and of 20 simulations from the full ensemble of 50 simulations and analyzing the crossing angle distributions for each subset (Figure 8A). This suggested that running smaller ensembles could result in a biased view of the helix packing model. Thus, for the single $N = 10$ subset, the randomly selected frequency of right-handed crossing was slightly less than that for the left handed packing of the helices.

To approach this more systematically, we next performed a jackknife analysis of the $N = 50$ ensemble. On the basis of this analysis, we could estimate the convergence of, e.g., the probability of a right-handed helix packing and of the crossing


dx.doi.org/10.1021/ct500003g | J. Chem. Theory Comput. 2014, 10, 2165−2175

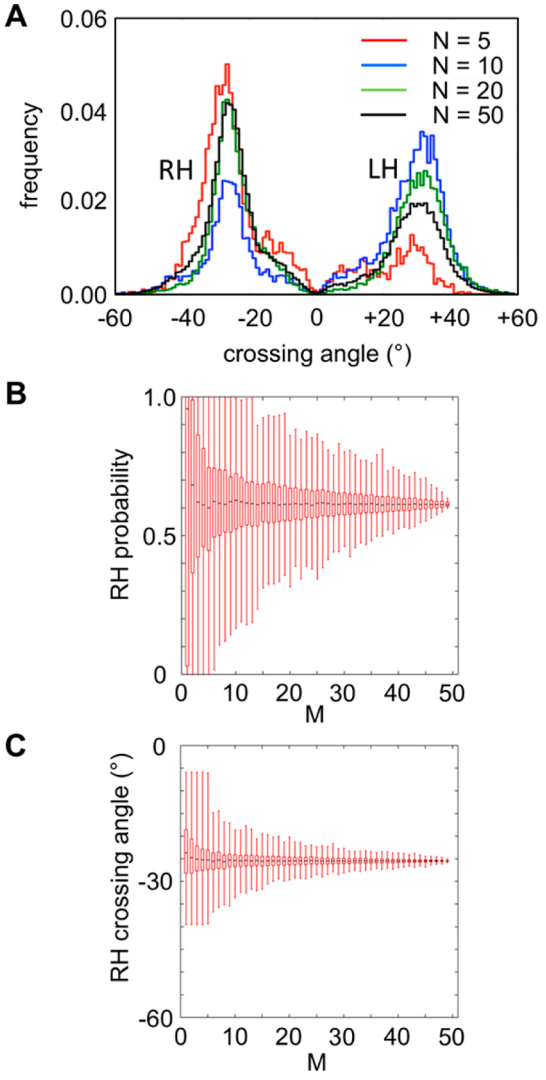


**Figure 8.** Convergence analysis of the ErbB1 TM helix dimerization ensemble. (A) Helix crossing angle distributions for different ensembles sizes ($N$ = 5, 10, 20, and 50). Both the $N$ = 20 and $N$ = 50 ensembles demonstrate clearly the preference for right-handed (RH) over left handed (LH) dimer packing. (B and C) Results of jackknife analysis (see text for details) for the estimated probability (B) and mean crossing angle (C) for the RH packing mode as a function of the subset ensemble size $M$ (where a sample of 1000 ensembles of size $M$ are taken as subsets from the $N$ = 50 ensemble).

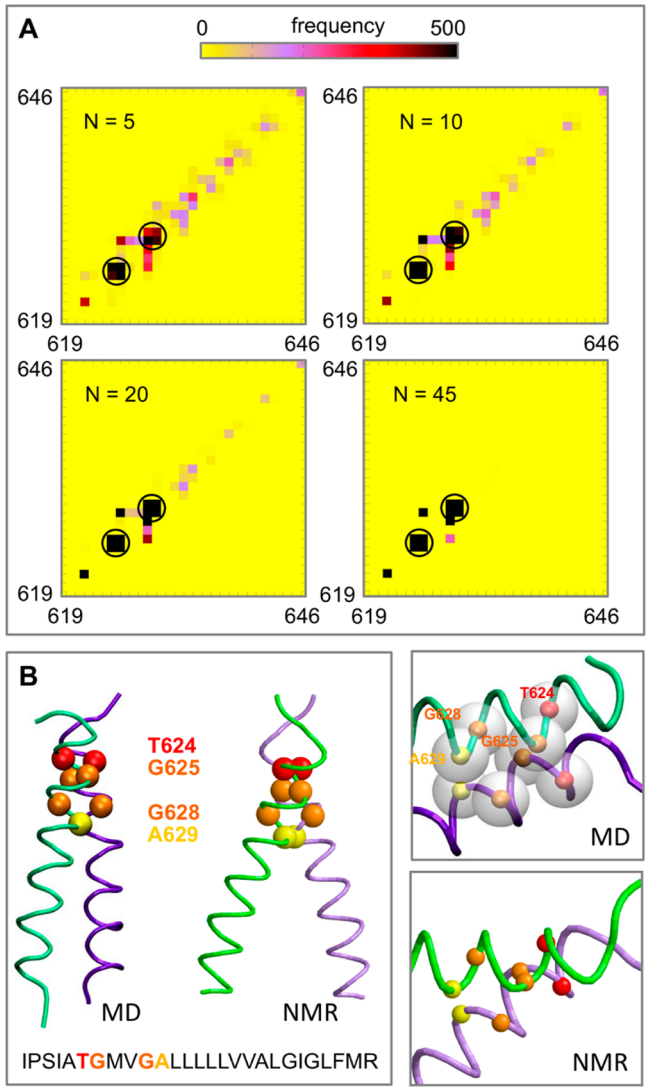


**Figure 9.** Analysis of ErbB1 TM helix dimer interactions. (A) Convergence analysis of the ErbB1 TM helix–helix contact interactions for the RH packing mode via jackknife analysis for different ensemble sizes ($N$ = 5, 10, 20, and 45) drawn from the 50 simulations. The helix interactions are shown on a contact matrix where the heatscale indicates the relative frequency of interactions. Circles indicate the interactions observed for the small–small-x-x-small–small motif (T624-G625-x-x-G628-A629) in the NMR structure of the ErbB1 TM-JM helix dimer.[37] (B) Representative structures of the RH and LH dimer populations with the T624 and G628 contact residues (in red) shown along with the sequence of the ErbB1 TM region.

angle for right-handed packing as a function of subensemble size $M$ (see Figure 8B,C for details). On the basis of this analysis, one can judge that reasonable convergence is attained after a subensemble size of ca. 20 or above. This is a valuable indication of what sizes of ensembles to generate if Sidekick or related methodologies are used to explore different families of related TM helix dimers via CG simulations.[66]

We extended this analysis to that of convergence of the residues involved in the ErbB1 TM-TM packing interactions. Thus, we used jackknife analysis to explore convergence of the helix–helix contact matrix (Figure 9A). From this, we can see convergence to a preferred motif ("top 10 contacts") corresponding to symmetrical interactions of residues T624, G625, G628, and A629 in the two TM helices. As with the helix crossing angle distributions, convergence seems to be achieved for subensembles of $N$ = 20 or above. If one selects a representative structure from the ensemble, the resultant structure agrees well with those from NMR studies (Figure 9B). We note that the modal crossing angle from our CG simulations (ca. −26°) is a little smaller than that for the recent NMR structure (ca. −44°). This difference is likely to reflect the absence of the juxtamembrane region from the model of the ErbB1 TM domain used in our simulations and possibly also the difference between a DPPC bilayer (used in our simulations) and a DHPC/DMPC bicelle (used in the NMR experiments). We further note that this difference is comparable to the variation observed between alternative experiments on the influenza M2 proton channel.[67]


dx.doi.org/10.1021/ct500003g | J. Chem. Theory Comput. 2014, 10, 2165−2175

## CONCLUSIONS

We have demonstrated the utility of the Sidekick pipeline for the running and analysis of CG-MD simulations of TM helices. This approach enhances our ability to run high throughput simulations of large ensembles of TM helices and thus to explore biophysical properties of model membrane systems. Such high throughput approaches to biophysics are becoming increasingly commonplace, and their increased automation is a key element facilitating more widespread adoption.[12,27] Thus, approaches such as Sidekick will enable, e.g., integration of simulation studies within experimental workflows.

The application of Sidekick to analyzing Arg residue positional effects on TM helix insertion into bilayers exemplifies the need for automated simulations to enable analysis and comparisons of large ensembles of different simulations. The results of a systematic survey of arginine-containing single helices reproduce available experimental and simulation data and extend our understanding of the fundamental interactions underlying membrane protein folding and assembly.

We have further demonstrated that Sidekick-enabled ensemble simulations are capable of predicting the interactions of the TM regions of ErbB1, and we have highlighted the importance of a more formal analysis of convergence of helix packing models, which can be achieved using an automated approach. This is of special importance if CGMD and multiscale simulation based modeling are to complement experimental, e.g., NMR, studies in allowing us to understand TM domain conformational dynamics in RTKs and related receptor proteins. The success of the application to the ErbB1 homodimer shows that Sidekick offers a platform for performing systematic "parameter sweeps" of TM helix dimerization. While we have exclusively examined CG systems here, the approach could equally apply to all atom approaches with sufficient computing power or multiscale approaches.[6] Such extensions are supported by the wide use of object oriented programming and modular design of the pipelines, allowing for new functions and behaviors to be added relatively easily. In this way, it should be possible to explore, e.g., changes in structure and stability of dimerization across extended families of TM helices from receptors.[66]

Future studies will include the development of increasingly complex pipelines which allow the analysis of distinct properties and larger systems. For transmembrane helices, a valuable addition to the pipelines would be the ability to perform energy calculations (e.g., potential of mean force calculations, steered molecular dynamics, or thermodynamic integration). Preliminary studies have shown that it is possible to add an umbrella potential to single helix simulations, demonstrating that potentials of mean force may be calculated through relatively small modifications to the pipeline. Similarly, the ability to convert between coarse grained and atomistic representations[6] within a pipeline will add to the usefulness of the tool in future.

The applications of automated simulation extend beyond transmembrane helices. Future efforts will involve the expansion of the types of system which can be studied. Coarse grained nucleic acid/lipid interactions[68] represent a natural future target for pipelined simulations. Protein−protein interactions[69] and protein−membrane interactions[70] also present an attractive goal but will require advances in the development of more generic metrics to describe the motions and interactions within these more complex systems and may require more powerful machine learning approaches for understanding the resulting aggregated data. The future of pipelined simulations therefore promises the ability to make biomolecular simulations easier and more reproducible across a broad range of different domains.

## ASSOCIATED CONTENT

### Supporting Information

Sidekick hardware architecture and the dynamics of a single L11 helix insertion simulation (see Figure 4 and Table 1 for details). This material is available free of charge via the Internet at http://pubs.acs.org.

## AUTHOR INFORMATION

### Corresponding Author

*E-mail: mark.sansom@bioch.ox.ac.uk.

### Present Address

[†]B.A.H.: Microsoft Research Cambridge, 21 Station Road, Cambridge CB1 2FB, U.K.

### Funding

We thank the BBSRC and the Wellcome Trust for support. K.B.A.H. is supported by The Khazanah-OCIS Merdeka Scholarship Program.

### Notes

The authors declare no competing financial interest.

## REFERENCES

(1) Lindahl, E.; Sansom, M. S. P. Membrane proteins: molecular dynamics simulations. *Curr. Opin. Struct. Biol.* **2008**, *18*, 425−431.

(2) Freddolino, P. L.; Arkhipov, A. S.; Larson, S. B.; McPherson, A.; Schulten, K. Molecular dynamics simulations of the complete satellite tobacco mosaic virus. *Structure* **2006**, *14*, 437−449.

(3) Schäfer, L. V.; de Jong, D. H.; Holt, A.; Rzepiela, A. J.; de Vries, A. H.; Poolman, B.; Killian, J. A.; Marrink, S. J. Lipid packing drives the segregation of transmembrane helices into disordered lipid domains in model membranes. *Proc. Natl. Acad. Sci. U.S.A.* **2011**, *108*, 1343−1348.

(4) Johansson, A. C. V.; Lindahl, E. Protein contents in biological membranes can explain abnormal solvation of charged and polar residues. *Proc. Natl. Acad. Sci. U.S.A.* **2009**, *106*, 15684−15689.

(5) Dror, R. O.; Jensen, M. Ø.; Borhani, D. W.; Shaw, D. E. Exploring atomic resolution physiology on a femtosecond to millisecond timescale using molecular dynamics simulations. *J. Gen. Physiol.* **2010**, *135*, 555−562.

(6) Stansfeld, P. J.; Sansom, M. S. P. From coarse-grained to atomistic: a serial multi-scale approach to membrane protein simulations. *J. Chem. Theor. Comput.* **2011**, *7*, 1157−1166.

(7) Sansom, M. S. P.; Scott, K. A.; Bond, P. J. Coarse grained simulation: a high throughput computational approach to membrane proteins. *Biochem. Soc. Trans.* **2008**, *36*, 27−32.

(8) Chetwynd, A. P.; Scott, K. A.; Mokrab, Y.; Sansom, M. S. P. CGDB: a database of membrane protein/lipid interactions by coarse-grained molecular dynamics simulations. *Mol. Membr. Biol.* **2008**, *25*, 662−669.

(9) Salwinski, L.; Eisenberg, D. Computational methods of analysis of protein-protein interactions. *Curr. Opin. Struct. Biol.* **2003**, *13*, 377−382.

(10) Richards, W. G. Virtual screening using grid computing: the screensaver project. *Nature Rev. Drug Discovery* **2002**, *1*, 551−555.

(11) Schuttelkopf, A. W.; van Aalten, D. M. F. PRODRG: a tool for high-throughput crystallography of protein-ligand complexes. *Acta Crystallogr., Sect. D* **2004**, *60*, 1355−1363.

(12) Harvey, M. J.; De Fabritiis, G. High-throughput molecular dynamics: the powerful new tool for drug discovery. *Drug Discovery Today* **2012**, *17*, 1059−1062.

(13) Barrett, C. P.; Noble, M. E. M. Dynamite extended: two new services to simplify protein dynamic analysis. *Bioinformatics* **2005**, *21*, 3174−3175.

(14) Gerstein, M.; Echols, N. Exploring the range of protein flexibility, from a structural proteomics perspective. *Curr. Opin. Chem. Biol.* **2004**, *8*, 14−19.
(15) Vohra, S.; Hall, B. A.; Holdbrook, D. A.; Khalid, S.; Biggin, P. C. Bookshelf: a simple curation system for the storage of biomolecular simulation data. *Database* **2010**, baq033.
(16) Hess, B.; Kutzner, C.; van der Spoel, D.; Lindahl, E. GROMACS 4: algorithms for highly efficient, load-balanced, and scalable molecular simulation. *J. Chem. Theor. Comput.* **2008**, *4*, 435−447.
(17) Kalé, L.; Skeel, R.; Bhandarkar, M.; Brunner, R.; Gursoy, A.; Krawetz, N.; Phillips, J.; Shinozaki, A.; Varadarajan, K.; Schulten, K. NAMD2: Greater scalability for parallel molecular dynamics. *J. Comput. Phys.* **1999**, *151*, 283−312.
(18) Brooks, B. R.; Bruccoleri, R. E.; Olafson, B. D.; States, D. J.; Swaminathan, S.; Karplus, M. CHARMM: A program for macromolecular energy, minimisation, and dynamics calculations. *J. Comput. Chem.* **1983**, *4*, 187−217.
(19) Scott, W. R. P.; Hunenberger, P. H.; Tironi, I. G.; Mark, A. E.; Billeter, S. R.; Fennen, J.; Torda, A. E.; Huber, T.; Kruger, P.; van Gunsteren, W. F. The GROMOS biomolecular simulation program package. *J. Phys. Chem. A* **1999**, *103*, 3596−3607.
(20) Pearlman, D. A.; Case, D. A.; Caldwell, J. W.; Ross, W. S.; Cheatham, T. E.; Debolt, S.; Ferguson, D.; Seibel, G.; Kollman, P. Amber, a package of computer-programs for applying molecular mechanics, normal-mode analysis, molecular-dynamics and free-energy calculations to simulate the structural and energetic properties of molecules. *Comput. Phys. Commun.* **1995**, *91*, 1−41.
(21) Bond, P. J.; Holyoake, J.; Ivetac, A.; Khalid, S.; Sansom, M. S. P. Coarse-grained molecular dynamics simulations of membrane proteins and peptides. *J. Struct. Biol.* **2007**, *157*, 593−605.
(22) DeVane, R.; Shinoda, W.; Moore, P. B.; Klein, M. L. Transferable coarse grain nonbonded interaction model for amino acids. *J. Chem. Theor. Comput.* **2009**, *5*, 2115−2124.
(23) Monticelli, L.; Kandasamy, S. K.; Periole, X.; Larson, R. G.; Tieleman, D. P.; Marrink, S. J. The MARTINI coarse grained force field: extension to proteins. *J. Chem. Theor. Comput.* **2008**, *4*, 819−834.
(24) Anderson, D. P.; Cobb, J.; Korpela, E.; Lebofsky, M.; Werthimer, D. SETI@home - An experiment in public-resource computing. *Commun. ACM* **2002**, *45*, 56−61.
(25) Beberg, A. L.; Ensign, D. L.; Jayachandran, G.; Khaliq, S.; Pande, V. S. Folding@home: Lessons from Eight Years of Volunteer Distributed Computing. In *2009 IEEE International Symposium on Parallel & Distributed Processing*; IEEE: Washington, DC, 2009; Vol. *1*−*5*, pp 1624−1631.
(26) Buch, I.; Harvey, M. J.; Giorgino, T.; Anderson, D. P.; De Fabritiis, G. High-throughput all-atom molecular dynamics simulations using distributed computing. *J. Chem. Inf. Model.* **2010**, *50*, 397−403.
(27) Pronk, S.; Larsson, P.; Pouya, I.; Bowman, G. R.; Haque, I. S.; Beauchamp, K.; Hess, B.; Pande, V. S.; Kasson, P. M.; Lindahl, E. In *Proceedings of 2011 International Conference for High Performance Computing, Networking, Storage and Analysis (SC '11)*; ACM: New York, 2011.
(28) Vostrikov, V. V.; Hall, B. A.; Greathouse, D. V.; Koeppe, R. E.; Sansom, M. S. P. Changes in transmembrane helix alignment by arginine residues revealed by solid-state NMR experiments and coarse-grained MD simulations. *J. Am. Chem. Soc.* **2010**, *132*, 5803−5811.
(29) Vostrikov, V. V.; Hall, B. A.; Sansom, M. S. P.; Koeppe, R. E. Accommodation of a central arginine in a transmembrane peptide by changing the placement of anchor residues. *J. Phys. Chem. B* **2012**, *116*, 12980−12990.
(30) Hall, B. A.; Chetwynd, A.; Sansom, M. S. P. Exploring peptide-membrane interactions with coarse grained MD simulations. *Biophys. J.* **2011**, *100*, 1940−1948.
(31) Hall, B. A.; Armitage, J. P.; Sansom, M. S. P. Mechanism of bacterial signal transduction revealed by molecular dynamics of Tsr dimers and trimers of dimers in lipid vesicles. *PLoS Comp. Biol.* **2012**, *8*, e1002685.
(32) Lindau, M.; Hall, B. A.; Chetwynd, A.; Beckstein, O.; Sansom, M. S. P. Coarse-grain simulations reveal movement of the synaptobrevin C-terminus in response to piconewton forces. *Biophys. J.* **2012**, *103*, 959−969.
(33) Crowet, J. M.; Parton, D. L.; Hall, B. A.; Steinhauer, S.; Brasseur, R.; Lins, L.; Sansom, M. S. P. Multi-scale simulation of the simian immunodeficiency virus fusion peptide. *J. Phys. Chem. B* **2012**, *116*, 13713−13721.
(34) Moon, C. P.; Fleming, K. G. Side-chain hydrophobicity scale derived from transmembrane protein folding into lipid bilayers. *Proc. Natl. Acad. Sci. U.S.A.* **2011**, *108*, 10174−10177.
(35) Hessa, T.; Meindl-Beinker, N. M.; Bernsel, A.; Kim, H.; Sato, Y.; Lerch-Bader, M.; Nilsson, I.; White, S. H.; von Heijne, G. Molecular code for transmembrane-helix recognition by the Sec61 translocon. *Nature* **2007**, *450*, 1026−U2.
(36) Ulmschneider, M. B.; Doux, J. P. F.; Killian, J. A.; Smith, J. C.; Ulmschneider, J. P. Mechanism and kinetics of peptide partitioning into membranes from all-atom simulations of thermostable peptides. *J. Am. Chem. Soc.* **2010**, *132*, 3452−3460.
(37) Endres, N. F.; Das, R.; Smith, A. W.; Arkhipov, A.; Kovacs, E.; Huang, Y. J.; Pelton, J. G.; Shan, Y. B.; Shaw, D. E.; Wemmer, D. E.; Groves, J. T.; Kuriyan, J. Conformational coupling across the plasma membrane in activation of the EGF receptor. *Cell* **2013**, *152*, 543−556.
(38) Berendsen, H. J. C.; Postma, J. P. M.; van Gunsteren, W. F.; DiNola, A.; Haak, J. R. Molecular dynamics with coupling to an external bath. *J. Chem. Phys.* **1984**, *81*, 3684−3690.
(39) Winger, M.; Trzesniak, D.; Baron, R.; van Gunsteren, W. F. On using a too large integration time step in molecular dynamics simulations of coarse-grained molecular models. *Phys. Chem. Chem. Phys.* **2009**, *11*, 1934−1941.
(40) Marrink, S. J.; Periole, X.; Tieleman, D. P.; de Vries, A. H. Comment on "On using a too large integration time step in molecular dynamics simulations of coarse-grained molecular models" by Winger, M.; Trzesniak, D.; Baron, R.; W. F. van Gunsteren *Phys. Chem. Chem. Phys.*, **2009**, *11*, 1934. *Phys. Chem. Chem. Phys.* **2010**, *12*, 2254−2256.
(41) Kalli, A.; B.A, H.; Campbell, I. D.; Sansom, M. S. P. A helix heterodimer in a lipid bilayer: structure prediction of the structure of an integrin transmembrane domain via multiscale simulations. *Structure* **2011**, *19*, 1477−1484.
(42) Lämmel, R. Google's MapReduce programming model - revisited. *Sci. Comp. Prog.* **2008**, *70*, 1−30.
(43) Lindahl, E.; Hess, B.; van der Spoel, D. GROMACS 3.0: a package for molecular simulation and trajectory analysis. *J. Mol. Model.* **2001**, *7*, 306−317.
(44) Marrink, S. J.; Risselada, J.; Yefimov, S.; Tieleman, D. P.; de Vries, A. H. The MARTINI forcefield: coarse grained model for biomolecular simulations. *J. Phys. Chem. B* **2007**, *111*, 7812−7824.
(45) Psachoulia, E.; Marshall, D.; Sansom, M. S. P. Molecular dynamics simulations of the dimerization of transmembrane $\alpha$-helices. *Acc. Chem. Res.* **2010**, *43*, 388−396.
(46) Wilke, M. An iterative jackknife approach for assessing reliability and power of fMRI group analyses. *PLoS One* **2012**, *7*, e35578.
(47) Confalonieri, R.; Acutis, M.; Bellocchi, G.; Genovese, G. Resampling-based software for estimating optimal sample size. *Environ. Model. Software* **2007**, *22*, 1796−1800.
(48) White, S. H.; von Heijne, G. Transmembrane helices before, during, and after insertion. *Curr. Opin. Struct. Biol.* **2005**, *15*, 378−386.
(49) White, S. H.; von Heijne, G. How translocons select transmembrane helices. *Annu. Rev. Biophys.* **2008**, *37*, 23−42.
(50) Hessa, T.; Kim, H.; Bihlmaier, K.; Lundin, C.; Boekel, J.; Andersson, H.; Nilsson, I.; White, S. H.; von Heijne, G. Recognition of transmembrane helices by the endoplasmic reticulum translocon. *Nature* **2005**, *433*, 377−381.
(51) Doherty, T.; Su, Y.; Hong, M. High-resolution orientation and depth of insertion of the voltage-sensing S4 helix of a potassium channel in lipid bilayers. *J. Mol. Biol.* **2010**, *401*, 642−652.
(52) Tiriveedhi, V.; Miller, M.; Butko, P.; Li, M. Autonomous transmembrane segment S4 of the voltage sensor domain partitions into the lipid membrane. *Biochim. Biophys. Acta* **2012**, *1818*, 1698−1705.

(53) Chetwynd, A.; Wee, C. L.; Hall, B. A.; Sansom, M. S. P. The energetics of transmembrane helix insertion into a lipid bilayer. *Biophys. J.* **2010**, *99*, 2534−2540.
(54) Ulmschneider, M. B.; Smith, J. C.; Ulmschneider, J. P. Peptide partitioning properties from direct insertion studies. *Biophys. J.* **2010**, *98*, L60−L62.
(55) Dorairaj, S.; Allen, T. W. Free energies of arginine-lipid interactions: potential of mean force of a transmembrane helix through a membrane. *Biophys. J.* **2006**, *90*, 1022−Pos.
(56) Bond, P. J.; Wee, C. L.; Sansom, M. S. P. Coarse-grained molecular dynamics simulations of the energetics of helix insertion into a lipid bilayer. *Biochemistry* **2008**, *47*, 11321−11331.
(57) Schow, E. V.; Freites, J. A.; Cheng, P.; Bernsel, A.; von Heijne, G.; White, S. H.; Tobias, D. J. Arginine in membranes: the connection between molecular dynamics simulations and translocon-mediated insertion experiments. *J. Membr. Biol.* **2011**, *239*, 35−48.
(58) Li, L. B.; Vorobyov, I.; Allen, T. W. The different interactions of lysine and arginine side chains with lipid membranes. *J. Phys. Chem. B* **2013**, *117*, 11906−11920.
(59) Fry, W. H. D.; Kotelawala, L.; Sweeney, C.; Carraway, K. L. Mechanisms of ErbB receptor negative regulation and relevance in cancer. *Exp. Cell Res.* **2009**, *315*, 697−706.
(60) Normanno, N.; De Luca, A.; Bianco, C.; Strizzi, L.; Mancino, M.; Maiello, M. R.; Carotenuto, A.; De Feo, G.; Caponigro, F.; Salomon, D. S. Epidermal growth factor receptor (EGFR) signaling in cancer. *Gene* **2006**, *366*, 2−16.
(61) Lemmon, M. A.; Treutlein, H. R.; Adams, P. D.; Brunger, A. T.; Engelman, D. M. A dimerisation motif for transmembrane a helices. *Nat. Struct. Biol.* **1994**, *1*, 157−163.
(62) Mineev, K. S.; Bocharov, E. V.; Pustovalova, Y. E.; Bocharova, O. V.; Chupin, V. V.; Arseniev, A. S. Spatial structure of the transmembrane domain heterodimer of ErbB1 and ErbB2 receptor tyrosine kinases. *J. Mol. Biol.* **2010**, *400*, 231−243.
(63) Prakash, A.; Janosi, L.; Doxastakis, M. Self-association of models of transmembrane domains of ErbB receptors in a lipid bilayer. *Biophys. J.* **2010**, *99*, 3657−3665.
(64) Prakash, A.; Janosi, L.; Doxastakis, M. GxxxG motifs, phenylalanine, and cholesterol guide the self-association of transmembrane domains of ErbB2 receptors. *Biophys. J.* **2011**, *101*, 1949−1958.
(65) MacKenzie, K. R.; Prestegard, J. H.; Engelman, D. M. A transmembrane helix dimer: structure and implications. *Science* **1997**, *276*, 131−133.
(66) Finger, C.; Escher, C.; Schneider, D. The single transmembrane domain of human tyrosine kinases encode self interactions. *Sci. Signaling* **2009**, *2* (ra56), 1−8.
(67) Cross, T. A.; Dong, H.; Sharma, M.; Busath, D. D.; Zhou, H.-X. M2 protein from influenza A: from multiple structures to biophysical and functional insights. *Curr. Opin. Virol.* **2012**, *2*, 128−133.
(68) Khalid, S.; Bond, P. J.; Holyoake, J.; Hawtin, R. W.; Sansom, M. S. P. DNA and lipid bilayers: self assembly and insertion. *J. R. Soc. Interface* **2008**, *5*, S241−S250.
(69) Hall, B. A.; Sansom, M. S. P. Coarse-grained MD simulations and protein-protein interactions: the cohesin-dockerin system. *J. Chem. Theor. Comput.* **2009**, *5*, 2465−2471.
(70) Kalli, A. C.; Devaney, I.; Sansom, M. S. P. Interactions of phosphatase and tensin homologue (PTEN) proteins with phosphatidylinositol phosphates: insights from molecular dynamics simulations of PTEN and voltage sensitive phosphatase. *Biochemistry* **2014**, *53*, 1724−1732.